Solvothermal synthesis of Au@Fe$_3$O$_4$ nanoparticles for antibacterial applications

Zhazgul Kelgenbaeva[1,*], *Zhypargul* Abdullaeva[2], and *Bektemir* Murzubraimov[1]

[1]Institute of Chemistry and Phytotechnology, National Academy of Sciences of the Kyrgyz Republic, 720071 Bishkek, Kyrgyzstan
[2]Department of Material Sciences and Engineering, Kumamoto University, 860-8555 Kumamoto, Japan

Abstract. We present Au@Fe$_3$O$_4$ nanoparticles obtained from Fe nanoparticles and HAuCl$_4$ using a simple solvothermal method. Trisodium citrate ($C_6H_5Na_3O_7 \ast 2H_2O$) served as a reducing agent for Au. X-ray diffraction analysis, electronic microscopes and energy-dispersive X-ray spectroscopy revealed cubic structure, elemental composition (Au, Fe and O) and spherical shape of nanoparticles. Antibacterial activity of the sample was tested against *E. coli* bacteria and obtained results were discussed.

1 Introduction

Bimetallic nanoparticles have recently attracted much attention, because of their unique catalytic, electronic, optical, magnetic and other novel dual (depending on metals) properties and wide range of possible applications [1]. In particular, binary 3d-5d nanoparticles formed by transition metals such as Fe or Co together with 5d noble metals such as Au or Pt allow the possibility to tune the magnetic properties based on an in-depth knowledge of their geometrical and magnetic behaviour [2-3]. The bimetallic nanoparticles are generally divided into two types in the structure: the alloyed and the core/shell structured bimetallic nanoparticles [4].

Concerning the synthesis of Au@Fe$_3$O$_4$ nanoparticles, Seino et al. [5] synthesized magnetic carriers consisting of nano iron oxide and gold core-shell structure in an aqueous solution by using γ–ray irradiation. Lyon et al. [6] prepared core-shell structures with gold coating layers on the surface of either Fe$_2$O$_3$ or partially oxidized Fe$_3$O$_4$ via iteration hydroxylamine seeding. Yu et al. [7] also synthesized the so-called dumbbell-like Au-Fe$_3$O$_4$ bifunctional nanoparticles with interesting novel properties.

Among existed techniques [8-9], solvothermal synthesis can be one of the simplest and environmentally friendly ways for preparation of bimetallic nanomaterials [10]. The method is based on chemical reaction between initial substances and solvent mixture, and being heated at temperatures from 100 to 1000 °C, and pressure starting from 1 MPa. Solvothermal reaction takes place inside the stainless steel autoclave, covered by stainless steel lid, and fixed tightly by screws. Experimental conditions of this method can be varied

---

* Corresponding author: jaza-86@mail.ru

and allow to synthesize different types of materials. In this work, Au@Fe$_3$O$_4$ bimetallic nanoparticles were synthesized from the mixture of Fe nanoparticles with HAuCl$_4$ solution using solvothermal reaction and their properties were studied. For biomedical applications, synthesized Au@Fe$_3$O$_4$ nanoparticles were tested against Escherichia coli bacteria. *E. coli*, a gram-negative bacterium can enter human intestines and cause urinary tract infection, cholecystitis, or septicaemia [11].

2 Experimental

Experimental setup presented in Figure 1a was used for Au@Fe$_3$O$_4$ nano-sample preparation. Fe nanoparticles with an average diameter of 5 nm, synthesized by pulsed plasma in liquid method [12], were used as Fe sources. Teflon cup (total volume of 60 mL) was filled with Fe nanoparticles, 1.0 mM tetracloroauric acid (HAuCl$_4$) as Au source, Trisodium Citrate Dehydrate (TCD: C$_6$H$_5$Na$_3$O$_7$*2H$_2$O) as a reducing agent for Au nanoparticles and deionized water. Experimental conditions were as following the temperature T = 150 °C, pressure P =1.8 MPa and reaction time t = 2 hours. After the reaction, the temperature of autoclave cooled to room temperature and the liquid was taken out of the autoclave. The colour of the liquid changed from transparent to bright brown, sample was separated from the liquid, dried and then characterized. The starting materials, experimental conditions and process of the nanoparticles' formation are schematically represented in Figure 1b.

The sample was characterized by X-ray diffraction (XRD) performed on a Rigaku RINT-2500 HV diffractometer (Cu- Kα radiation, λ= 0.15406 nm; voltage of 40 kV, and current of 200 mA). Surface view and elemental composition analysis were examined by JEOL JSM-7600F Field-Emission Scanning Electron Microscope (FE-SEM) equipped with an Energy-Dispersive X-ray Spectroscopy (EDS) operated at 200 keV. High-resolution transmission electronic microscopy (HR-TEM) with a Philips Tecnai F20S-Twin instrument was used to determine the size and morphology of the nanoparticles at 200 keV. For analysis the particles dispersed in ethanol were drop cast onto a carbon-film-coated copper grid, followed by evaporation and drying.
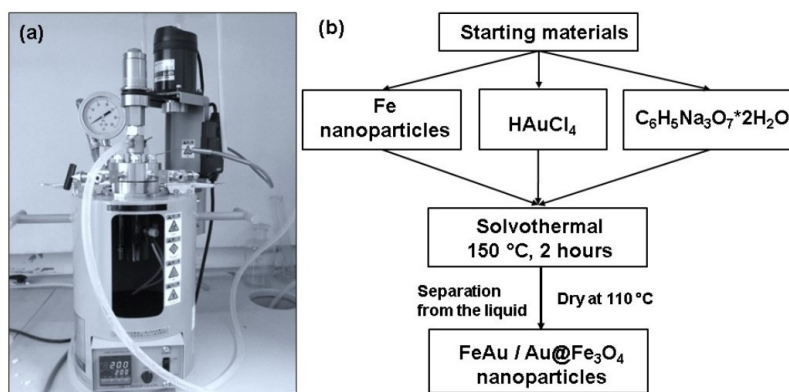

Fig. 1. a) Experimental setup of solvothermal method; b) Au@Fe$_3$O$_4$ nanoparticles preparation process by solvothermal synthesis

3 Results and Discussion

XRD is a rapid analytical technique primarily used for phase identification of a crystalline material and can provide information on unit cell dimensions. Figure 2 shows an XRD pattern of the Au-Fe bimetallic nano-sample. The diffration peaks at (2Θ) 38.180, 44. 658, 64. 542, 77. 536 and 82. 300 were attributed to gold, which can be indexed to (111), (200), (220), (311) and (222) lattice planes of gold in cubic phase Fm-3m (JCPDS card no 04-0784). The peaks at (2Θ) 30.167, 35. 336, 36.136, 43.255, 57.382, 62. 595, 65.00, 89. 617 were identified as magnetite ($Fe+2Fe_2+3O_4$) with cubic spinel (Fd-3m) structure (JCPDS card no 19-0629), indicating the presence of both Fe_3O_4 (magnetite) and Au (gold) in the sample.
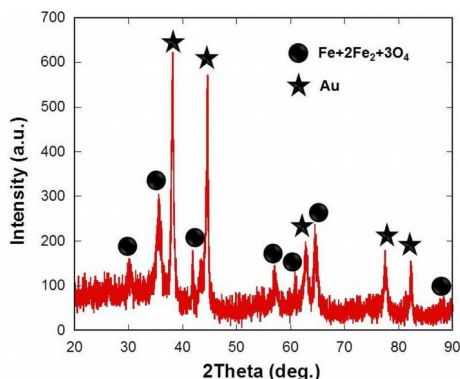

Fig. 2. X-Ray diffraction pattern of Au@Fe_3O_4 nanoparticles synthesized by solvothermal method

Further, the evidence for the presence of Au and Fe_3O_4 in the sample was proved by EDS, as shown in Figure 3 (left), where the elements gold (Au), iron (Fe), and oxygen (O) have been detected. The composition of the magnetite phase (Fe_3O_4) is 43 at% of iron and 57 at% of oxygen. In addition, peaks belonging to sodium (Na), chlorine (Cl) and carbon (C) were detected due to the reducing agent (TCD) and sample holding carbon tape.
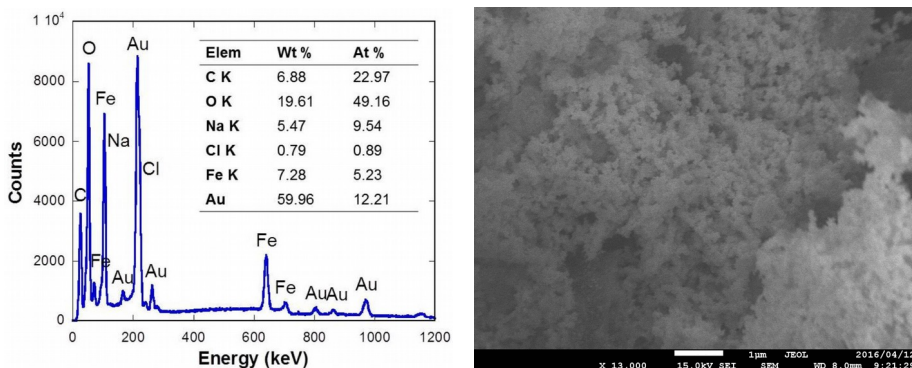

Fig. 3. Elemental composition and microphotography of Au@Fe_3O_4 nanoparticles synthesized by solvo-thermal synthesis

3

Surface view of the Au@Fe$_3$O$_4$ nanoparticles taken by FE-SEM is presented on microphotography on the right (Figure 3). Image was captured at resolution of ×13000, and the agglomerates are clearly displayed. Because of the high surface energy of the nanoparticles and chemical bonds between the particle's surfaces, their tendency to form agglomerates is quite strong. Magnetic dipole forces also potentially contribute to inter-particulate forces [13]. As it can be seen from Figure 4 the size of obtained nanoparticles ranged between 10-13 nm.
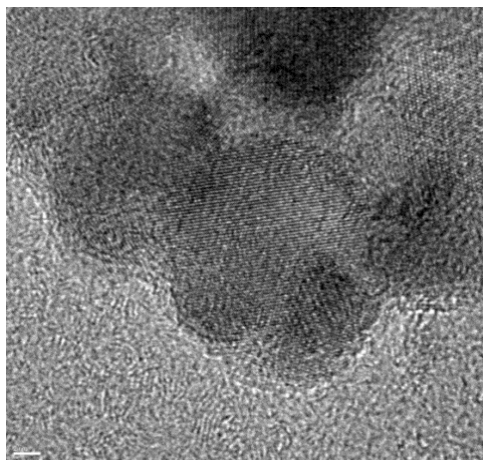

Fig. 4. HR-TEM image of several Au@Fe$_3$O$_4$ nanoparticles synthesized by solvothermal synthesis

Bacterial infections were one of the major causes of mortality in the nineteenth century. Nowadays, antimicrobial effects are intensively studied due to an enormously increasing bacterial resistance against excessively and repeatedly used classical antibiotics. Magnetic iron oxide nanoparticles are of particular interest as antibacterial agents, as they can be prepared with extremely high surface areas and unusual crystalline morphologies with a high number of edges and corners, and other potentially reactive sites [14]. Also, inorganic antibacterial agents such as metal and metal oxides are advantageous compared to organic compounds due to their stability. Ismail et al. studied that iron oxide nanoparticles with antibacterial properties and superparamagnetic nature are very prominent in biomedicine [15]. Antibacterial activity of the Au@Fe$_3$O$_4$ sample prepared by solvothermal synthesis was tested against *E coli* bacteria. Inhibition effect of the nanoparticles against the target microorganism was evaluated using 3M Petrifilm *E coli* / Coliform Count plates and inhibition time was 24 hours. Number of colonies were counted using the technique called TNTC (too numerous to count) and the results are represented in Table 1.

Table 1. Antibacterial activity of Au@Fe$_3$O$_4$ nanoparticles synthesized by solvothermal method

Nano particles	1 % concentration			0.1 % concentration			Control
	Probe I	Probe II	Probe III	Probe I	Probe II	Probe III	350 counts
$Au@Fe_3O_4$	101	102	97	200	207	199	
	Average: 100 counts			Average: 202 counts			

Following results were obtained after an average *E. coli* bacteria colonies calculation: as for control sheet there are 350 counts ; at 0.1 % concentration of the nanoparticles in medium - 202 counts and at 1.0 % concentration of the nanoparticles in media the value was 100. As it can be seen from obtained results, the bacteria count number decreased with increase of the nanoparticles concentration in medium. This means that $Au@Fe_3O_4$ nanoparticles synthesized by solvothermal synthesis can inhibit bacteria growth indicating on their good antibacterial activity.

4 Conclusions

Magnetic $Au@Fe_3O_4$ nanoparticles were synthesized from Fe nanoparticles and $HAuCl_4$, using TCD as reducing agent by solvothermal synthesis method. XRD and EDS analysis indicated the presence of Fe_3O_4 and Au phases in the sample. The $Au@Fe_3O_4$ nanoparticles have potent antibacterial activity against E coli bacteria and the inhibitory effect increases with increasing the nanoparticles concentration. Obtained results highlighte possible biomedical applications of $Au@Fe_3O_4$ nanoparticles as biocompatible components of antibiotics as well as medicaments.

References

1. O N. Toshima and T. Yonezawa, New J Chem., **22**, 1179-1201 (1998).
2. G. Rollman, M. E. Gruner, A. Hucht, R. Meyer, P. Entel, M. L. Tiago and J. R. Chelikowsky. Phys. Rev. Lett. **99**, 083402 (2007).
3. R. Singh and P. Kroll, Phys. Rev. **B 78**, 245404 (2008).
4. A. Zaleska-Medynska, M. Marchelek, M. Diak and E. Grabowska, Adv in Colloid and Interface Scie., **229,** 80-107 (2016).
5. S. Seino, T. Kinoshita, T. Nakagawa, T. Kojima, R. Taniguchi, S. Okuda and T. Yamamoto, J Nanopart Res., **10**, 1071-76 (2008).
6. J. L. Lyon, D. A. Fleming, M. B. Stone, P. Shiffer and M. E. Williams, Nano Let., **4,** 719-23 (2004).
7. H. Yu, M. Chen, P. M. Rice, S. X. Wang, R. L. White and S. Sun, Nano Let., **5**, 379-82 (2005).
8. H. Liu, P. Hou, W. Zhang, Y. K. Kim and J. Wu. Nanotechnology, **33,** 335602 (2010).
9. I. C. Chiang and D. H. Chen, Adv Functional Mater., **17,** 1311-16 (2007).

10. H. Chen, S. M. Yu, D. Shin and J. Yoo, Nanoscale Res Lett., **5**, 217-223 (2010).
11. N. Allocati, M. Masulli, M. F. Alexeyev, C. D. Ilio, Int J Environ Res Public Health, **10,** 6235-6254 (2013).
12. Z. Kelgenbaeva, E. Omurzak, S Takebe, S. Sulaimakulova, Z. Abdullaeva, C Iwamoto and T. Mashimo, J Nanopart Res., **16,** 2603 (2014).
13. R. Bandyopadhyaya, W. Rong, S. K. Friedlander, Chem. Mater., **16**, 3147-3154 (2004).
14. V. Velmurugan, G. Arunachalam, V. Ravichandran, Archives of Appl. Sci. Res., **2**, 147-150 (2010).
15. R. A. Ismail, G. M. Sulaiman, S. A. Abdulrahman, T. R. Marzoog, Materials Sci Eng.:C **53**, 286-297 (2015).